Halogen Bond Energy

International Edition: DOI: 10.1002/anie.201906279
German Edition: DOI: 10.1002/ange.201906279

Spectroscopic Measurement of a Halogen Bond Energy

Xinxing Zhang, Gaoxiang Liu, Sandra Ciborowski, Wei Wang, Chu Gong, Yifan Yao, and Kit Bowen**

Dedicated to the 100th anniversary of Nankai University

Abstract: *Halogen bonding (XB) has emerged as an important bonding motif in supramolecules and biological systems. Although regarded as a strong noncovalent interaction, benchmark measurements of the halogen bond energy are scarce. Here, a combined anion photoelectron spectroscopy and density functional theory (DFT) study of XB in solvated Br^- anions is reported. The XB strength between the positively-charged σ-hole on the Br atom of the bromotrichloromethane (CCl_3Br) molecule and the Br^- anion was found to be 0.63 eV (14.5 kcal mol^{-1}). In the neutral complexes, $Br(CCl_3Br)_{1,2}$, the attraction between the free Br atom and the negatively charged equatorial belt on the Br atom of CCl_3Br, which is a second type of halogen bonding, was estimated to have interaction strengths of 0.15 eV (3.5 kcal mol^{-1}) and 0.12 eV (2.8 kcal mol^{-1}).*

Even though they are generally regarded as electron withdrawing groups, already covalently-bonded halogen atoms can in addition interact attractively and directionally by a non-covalent bond to neighbor nucleophiles such as lone pairs and anions.[1–4] This noncovalent interaction was first referred to as "halogen bonding" (XB) by Dumas and coworkers in 1976.[5,6] Halogen atoms have positive electrostatic potential regions on the opposite end of their σ bond due to polarizability; moreover, the equatorial sides of these atoms exhibit negative electrostatic potential belts.[7,8] The positive facial site was termed as "σ-hole" by Politzer et al. in 2007,[9] although, clearly it is only a positive partial charge present at this site and no full electron is missing in any orbital. The size of the σ-hole depends on the polarizability of the halogen atom, that is, I > Br > Cl > F, but it can also be tuned by other highly electron-withdrawing functional groups in the molecule.[2] While the positively-charged σ-hole interacts with nucleophiles, the negatively-charged equatorial belt interacts with electrophiles, resulting in two categories of XB interactions.[1] XB has rapidly expanded into applications such as crystal engineering.[10–14] It also has provoked the survey of biological structures, where XB has been found to stabilize inter- and intramolecular interactions that can further affect ligand binding, protein folding, and enzymatic reactions.[15] While presence of XB interactions in the condensed-phase materials and biological chemistry is well known, experimental investigations of XB in the gas phase have been scarce. Nevertheless, techniques such as molecular beam scattering,[16] rotational spectroscopy,[17–19] blackbody infrared radiative dissociation[20] and ion-mobility mass spectrometry have provided significant insight.[21] More recently, our group reported the stabilization of otherwise unstable anions by XB using gas-phase anion photoelectron spectroscopy.[22]

Theoretical calculations have also been widely used to investigate the nature and applications of XB.[1–4,23–28] Even though many levels of theory have estimated the strength of a long list of XBs to be in the range of 0.04–1.20 eV,[29] they have hardly been investigated experimentally. There is a dearth of experimental determinations of halogen bond strengths. Gas-phase measurements of isolated systems has unique advantages to provide XB strengths that are in undisturbed local environments. In the current paper, we present a gas-phase, mass spectrometric and photoelectron spectroscopic study of the archetypical Br^--bromotrichloromethane complexes. In CCl_3Br, the Br atom exhibits a significant σ-hole, making it a good XB donor. The bromine anion is necessary to act as a negatively-charged non-covalent binding partner and to be able to apply the anion photoelectron spectroscopy. We measured the photoelectron spectra of $Br^-(CCl_3Br)_{0–2}$, and utilized density functional theory (DFT) calculations to compare with our experimental values, to visualize the XBs, and to provide thermodynamic rationales to understand the formation of these complexes.

Details of the experimental and theoretical methods are provided in the Supporting Information. The photoelectron spectra of Br^- and $Br^-(CCl_3Br)$ taken with 266 nm (4.66 eV) laser and $Br^-(CCl_3Br)_2$ taken with 193 nm (6.42 eV) laser are presented in Figure 1. The two peaks of Br^- at 3.37 eV and 3.82 eV correspond to the $^2P_{3/2}$ and $^2P_{1/2}$ spin-orbit states of the Br atom after photodetachment; these perfectly match reported values.[30] While their features are broadened, the anion photoelectron spectra of $Br^-(CCl_3Br)_{1,2}$ resemble the pattern seen in the spectrum of Br^-. This is because the Br^- moiety acts as the chromophore for photodetachment in both cases. Thus, $Br^-(CCl_3Br)_{1,2}$ are "solvated" anions, where Br^- is "solvated" by one and two CCl_3Br molecules, respectively. The electron binding energies (EBE) of the observed spectra

[*] Prof. Dr. X. Zhang, W. Wang, C. Gong, Y. Yao
Key Laboratory of Advanced Energy Materials Chemistry (Ministry of Education), Renewable Energy Conversion and Storage Center (ReCAST), College of Chemistry, Nankai University
Tianjin 300071 (China)
E-mail: zhangxx@nankai.edu.cn
Dr. G. Liu, S. Ciborowski, Prof. Dr. K. Bowen
Departments of Chemistry, Johns Hopkins University
Baltimore, MD 21218 (USA)
E-mail: kbowen@jhu.edu
Supporting information and the ORCID identification number(s) for the author(s) of this article can be found under: https://doi.org/10.1002/anie.201906279.

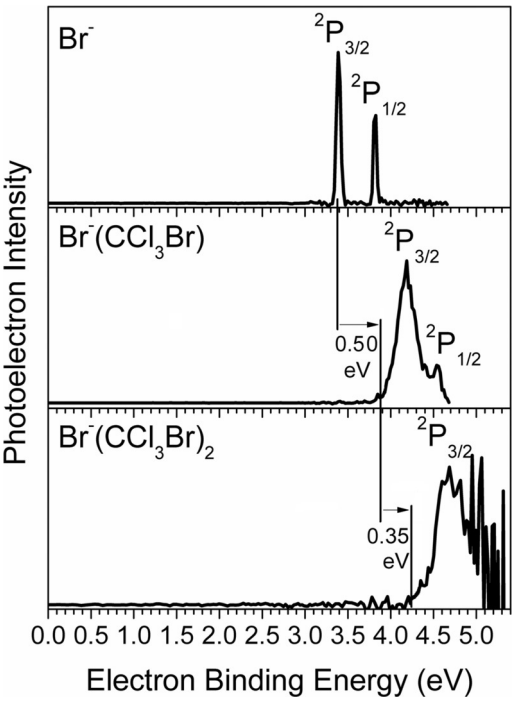

Figure 1. The photoelectron spectra of Br^- and $Br^-(CCl_3Br)$ taken with 266 nm (4.66 eV) photons and $Br^-(CCl_3Br)_2$ taken with 193 nm (6.42 eV) photons.

reflect the stabilization of the Br^- moiety's excess electron due to the solvation by CCl_3Br molecule(s). Their spectral broadening is likely due to vibrational motions that perturb the Br^- moiety. The persistence of the Br^- spectral pattern in the spectra of $Br^-(CCl_3Br)_1$ and $Br^-(CCl_3Br)_2$, even though the $^2P_{1/2}$ peak in the latter case is obscured by noise, implies good Franck–Condon overlap between the ground state of the anion and the ground state of the neutral. Ideally in such cases, the EBE threshold would provide the electron affinity (EA). Source conditions, however, often give rise to some degree of vibrational hot band intensity on the lowest EBE side of the origin peak. To account for this effect and thus to determine the EA value, we extrapolated the leading edge of the low EBE side of the peaks to zero intensity. These EBE values are 3.87 eV and 4.22 eV, and we report them as the experimentally-determined EA values of $Br(CCl_3Br)_{1,2}$, respectively. The EBE values of the intensity maxima in the main and lowest EBE peaks in these spectra correspond to their vertical detachment energies (VDE). Vertical detachment energies reflect the maximal Franck–Condon overlap between the anion and its neutral counterpart during photodetachment. The peak positions at EBE = 4.21 eV and 4.71 eV are the experimentally-determined vertical detachment energies (VDE) of of $Br^-(CCl_3Br)_1$ and $Br^-(CCl_3Br)_2$, respectively. As shown in Figure 1, the EA shifts between adjacent photoelectron spectra are 0.50 eV and 0.35 eV, respectively. These values are closely-related to the XB strength (see below). Table 1 presents both experimental and theoretical EA and VDE values for these systems. A high degree of consistency is seen there.

The calculated structures of $Br^{0/-}(CCl_3Br)_{1,2}$ and their highest occupied molecular orbitals (HOMO) are presented

Table 1: Experimental and theoretical EA values of $Br(CCl_3Br)_{0-2}$ and VDE values of $Br^-(CCl_3Br)_{1,2}$. All values are in eV.

	EA [Expt./Theo.]	VDE [Expt./Theo.]
$Br^{0/-}$	3.37/3.45	–
$Br^{0/-}(CCl_3Br)$	3.87/3.93	4.21/4.28
$Br^{0/-}(CCl_3Br)_2$	4.22/4.24	4.71/4.78

in Figure 2, and the 3D coordinates of all calculated species are presented in the Supporting Information. $Br^-(CCl_3Br)$ possesses a C_{3v} symmetry, where the Br atom in CCl_3Br and

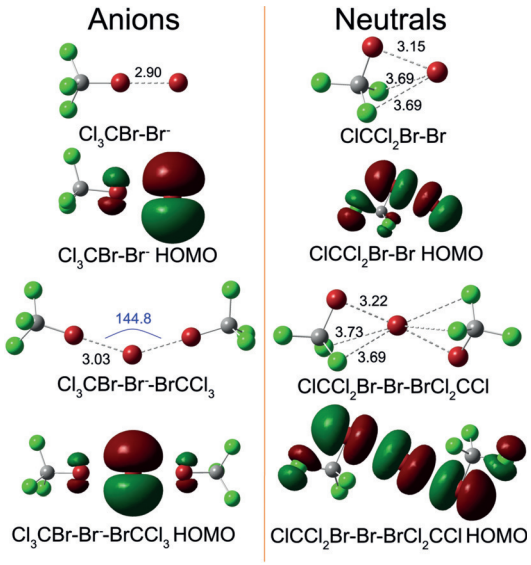

Figure 2. Calculated geometries and highest occupied molecular orbitals (HOMO) of $Br^{0/-}(CCl_3Br)_{1,2}$.

the Br^- kernel form a XB. Given this calculated structure, we write this complex as $Cl_3CBr\text{-}Br^-$. The XB length in $Cl_3CBr\text{-}Br^-$ is 2.90 Å, an indicator of a noncovalent bond. The HOMO of $Cl_3CBr\text{-}Br^-$, from which the photoelectron is detached, is mostly the *p* orbital of the Br^- kernel, consistent with the observed spectrum and its Br^- chromophore. For $Br^-(CCl_3Br)_2$, with a C_1 symmetry, the Br^- kernel is equally shared by two 3.03 Å long XB's. Likewise, we write $Br^-(CCl_3Br)_2$ as $Cl_3CBr\text{-}Br^-\text{-}BrCCl_3$. Since the negative charge on Br^- is shared by two CCl_3Br molecules, the electrostatic attraction is weakened compared to that in $Cl_3CBr\text{-}Br^-$, resulting in longer XB bonds. The HOMO of $Cl_3CBr\text{-}Br^-\text{-}BrCCl_3$ also shows a *p* orbital of Br^-. Interestingly, the two XBs exhibit a bond angle of 144.8°, even though intuitively they should be linear (see below). The neutral complexes exhibit very different structures. Compared to nucleophilic Br^-, a free Br atom is highly in need of one electron to fulfill the octet rule. Hence, being electrophilic in nature, the Br atom cannot form a conventional XB with the σ-hole, but tends instead to interact with the negatively-charged equatorial belt of Br and Cl atoms in CCl_3Br, forming the second type of XB. $Br(CCl_3Br)$ has a C_s symmetry, and $Br(CCl_3Br)_2$ has a C_1 symmetry. According to these structures, we write the neutrals as $ClCCl_2Br\text{-}Br$ and $ClCCl_2Br\text{-}Br\text{-}BrCl_2CCl$. The XB lengths in the neutrals are longer than those in the anions,

implying that the binding energy is weaker in the neutrals than in the anions. The HOMO's of $ClCCl_2Br$-Br and $ClCCl_2Br$-Br-$BrCl_2CCl$ clearly show the interaction between the *p* orbital of the free Br atom and the *p* orbital of the covalently bonded Br atom.

Natural population analysis (NPA) provides another perspective for understanding the solvation of the Br^- anion by $BrCCl_3$ molecule(s) via XB. The negative charge on the Br^- kernel is -0.80 *e* for Cl_3CBr-Br^- and -0.77 *e* for Cl_3CBr-Br^--$BrCCl_3$. Hence, a single XB interaction lowers the electron density on Br^- by -0.20 *e*, while two XB interactions further lower the charge by -0.03 *e*.

In order to better visualize XB, Figure 3 shows the electrostatic potential (ESP) surfaces of the anions, Cl_3CBr-Br^-, Cl_3CBr-Br^--$BrCCl_3$ (left) and the neutrals, CCl_3Br, $ClCCl_2Br$-Br and $ClCCl_2Br$-Br-$BrCl_2CCl$ (right). The induced positive (blue) and negative (red) electrostatic potentials are mapped on the 0.04 *e*/bohr^3 surfaces. In order to better visualize potential differences between spatial regions, the potentials ranging from -25 kcal mol^{-1} to $+50$ kcal mol^{-1} are presented for the anions, and potentials from -10 kcal mol^{-1} to $+150$ kcal mol^{-1} are presented for the neutrals. For the anionic Cl_3CBr-Br^- and Cl_3CBr-Br^--$BrCCl_3$, the XB between the σ-hole on the covalently-bonded Br atom (blue) and Br^- (red) can be clearly observed. On the equator of covalently-bonded Br and Cl atoms, there are negatively charged belts (red and yellow). To explore the 144.8° ∡BrBrBr bond angle in Cl_3CBr-Br^--$BrCCl_3$, we mapped the ESP of Cl_3CBr-Br^- on a different scale and from the axial perspective (lower left in Figure 3), where a less negatively-charged hole (yellow) on the non-XB side of Br^- is observed. The XB between Cl_3CBr and Br^- draws the negative charge on Br^- toward the XB, resulting in a less negatively-charged hole on the other side of Br^-. We tentatively refer to this electrostatic hole as the "halogen bond-hole" (XB-hole). In order to obtain the optimal electrostatic interaction, the XB formed with a second CCl_3Br avoids direct contact with this XB-hole, resulting in a ∡BrBrBr bond angle of 144.8° in Cl_3CBr-Br^--$BrCCl_3$. In neutral CCl_3Br (top right in Figure 3), even though

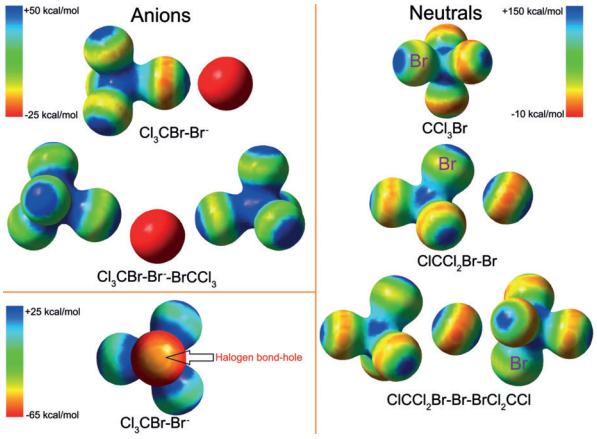

Figure 3. Electrostatic potential (ESP) surfaces for the anionic Cl_3CBr-Br^-, Cl_3CBr-Br^--$BrCCl_3$ (left) and neutral CCl_3Br, $ClCCl_2Br$-Br and $ClCCl_2Br$-Br-$BrCl_2CCl$ (right). The induced positive (blue), negative (red) potentials are mapped on the 0.04 *e*/bohr^3 surfaces of the molecules.

all the Cl and Br atoms exhibit σ-holes, due to its lower electronegativity and higher polarizability, the σ-hole on Br is larger than that on Cl, thus supporting the XB between Br and Br^- but not between Cl and Br^-. The evidence presented above overwhelmingly implies that the interactions between the Br^- anion and the CCl_3Br molecule(s) in the Br^--$(CCl3Br)_{1,2}$ anion complexes are dominated by halogen bonding. While electrostatic ion-dipole interactions no doubt contribute, they are expected to be minor by comparison, given the calculated small dipole moment of the CCl_3Br molecule (0.046 D).

For neutral $ClCCl_2Br$-Br and $ClCCl_2Br$-Br-$BrCl_2CCl$, the second type of halogen binding is observed, i.e., the interaction between the free electrophilic Br atom (see its blue region) and the negatively-charged equatorial belt of the covalently-bonded Br (reddish-yellow).

Next, we discuss the XB strengths. The strength of the first and second XB of the neutral and anionic complexes, $D_0[Br^{0/-}(CCl_3Br)_{1,2}]$, are calculated by

$$D_0[Br^{0/-}(CCl_3Br)] = E[Br^{0/-}] + E[CCl_3Br] - E[Br^{0/-}(CCl_3Br)] \quad (1)$$

and

$$D_0[Br^{0/-}(CCl_3Br)_2] = E[Br^{0/-}(CCl_3Br)] + E[CCl_3Br] - E[Br^{0/-}(CCl_3Br)_2], \quad (2)$$

where *E* refers to the calculated absolute energy of species with zero-point energy corrected. Our calculations found $D_0[Br^0(CCl_3Br)] = 0.15$ eV, $D_0[Br^-(CCl_3Br)] = 0.63$ eV, $D_0[Br^0(CCl_3Br)_2] = 0.12$ eV and $D_0[Br^-(CCl_3Br)_2] = 0.43$ eV. The binding energies of the anions are higher than those of the neutrals, consistent with bond length differences between the anionic and neutral complexes. Further,

$$D_0[Br^-(CCl_3Br)] - D_0[Br^0(CCl_3Br)] = (E[Br^0(CCl_3Br)] - E[Br^-(CCl_3Br)]) - (E[Br^0] - E[Br^-]) = EA[Br^0(CCl_3Br)] - EA[Br^0] \quad (3)$$

and

$$D_0[Br^-(CCl_3Br)_2] - D_0[Br^0(CCl_3Br)_2] = (E[Br^0(CCl_3Br)_2] - E[Br^-(CCl_3Br)_2]) - (E[Br^0(CCl_3Br)] - E[Br^-(CCl_3Br)]) = EA[Br^0(CCl_3Br)_2] - EA[Br^0(CCl_3Br)], \quad (4)$$

where EA denotes the electron affinity. Equations (3) and (4) show that the differences between the EAs of Br and $Br(CCl_3Br)$, and between the EAs of $Br(CCl_3Br)$ and Br-$(CCl_3Br)_2$ are equal to the binding energy differences between the anions and their neutral counterparts. In our photoelectron spectra (Figure 1), the EA shifts between adjacent size anionic species are 0.50 eV and 0.35 eV, respectively, in excellent agreement with the calculated binding energy differences, 0.48 eV and 0.31 eV.

The Gibbs free energy ΔG, that is, $\Delta G = \Delta H - T\Delta S$, has to be negative for a XB to form. The enthalpy change, ΔH, is negative, yet due to entropy decrease (loss of rotational and translational degrees of freedom) upon forming a XB, the $T\Delta S$ term often has a large negative value.[1] For this reason,

Table 2: Computed thermodynamic values (kcal mol^{-1}) for gas-phase XB complex formation. The maximum temperature (T*) at which each reaction to occur is also listed in units of K.

Reactions	ΔE^0	ΔH^0	$T\Delta S^0$	ΔG^0	T^*
$Br + CCl_3Br \rightarrow Br(CCl_3Br)$	−2.9	−3.5	−6.9	3.4	140
$Br^- + CCl_3Br \rightarrow Br^-(CCl_3Br)$	−3.9	−4.5	−6.6	−7.9	688
$Br(CCl_3Br) + CCl_3Br \rightarrow Br(CCl_3Br)_2$	−1.3	−1.9	−8.2	6.3	50
$Br^-(CCl_3Br) + CCl_3Br \rightarrow Br^-(CCl_3Br)_2$	−8.4	−9.0	−9.3	0.3	289

low temperatures are often required in order to form a XB in an isolated (gas-phase) environment. To better understand the formation of these complexes, the appropriate thermodynamic values computed at room temperature are tabulated in the first four columns of Table 2. The formation of the anions is more exothermic than the formation of the neutrals. At room temperature, only $Br^-(CCl_3Br)$ has a negative ΔG. The temperatures below which ΔG remains negative, T*, are also tabulated in Table 2. For $Br^-(CCl_3Br)$, ΔG is negative until the temperature reaches 688 K, this being largely due to the large enthalpy change despite the entropy loss. Thus, the formation of $Br^-(CCl_3Br)$ is favorable at temperatures below 688 K. The formation of $Br^-(CCl_3Br)_2$, on the other hand, cannot occur above 289 K. Likewise, the neutral molecules, $Br(CCl_3Br)_{1,2}$ can only be formed under 140 K and 50 K, respectively. Since supersonic expansions can form complexes with temperatures of several tens of degrees Kelvin,[31,32] the formation of all these species is thermodynamically allowed under the experimental conditions that obtained in these experiments.

To conclude, combined results from anion photoelectron spectroscopy and DFT calculations have shown the interaction between the Br^- anion and the CCl_3Br molecule(s) to be dominated by halogen bonding, XB. The halogen bonding interaction energy between Br^- and CCl_3Br in $Br^-(CCl_3Br)$ was determined to be 0.63 eV, thus providing a benchmark for the further exploration of halogen bonding in other systems.

Acknowledgements

This material is based upon work supported by the (U.S.) National Science Foundation under Grant No. CHE-1664182 (KHB). X. Z. acknowledges the College of Chemistry at Nankai University for the start funding.

Conflict of interest

The authors declare no conflict of interest.

Keywords: halogen bond · halogen bond energy · halogen-bond hole · photoelectron spectroscopy

How to cite: *Angew. Chem. Int. Ed.* **2019**, *58*, 11400–11403
Angew. Chem. **2019**, *131*, 11522–11525

[1] P. Politzer, J. S. Murray, T. Clark, *Phys. Chem. Chem. Phys.* **2013**, *15*, 11178–11189.
[2] P. Politzer, P. Lane, M. C. Concha, Y. Ma, J. S. Murray, *J. Mol. Model.* **2007**, *13*, 305–311.
[3] G. Cavallo, P. Metrangolo, R. Milani, T. Pilati, A. Priimagi, G. Resnati, G. Terraneo, *Chem. Rev.* **2016**, *116*, 2478–2601.
[4] M. H. Kolář, P. Hobza, *Chem. Rev.* **2016**, *116*, 5155–5187.
[5] J.-M. Dumas, M. Kern, J. L. Janier-Dubry, *Bull. Soc. Chim. Fr.* **1976**, 1785–1787.
[6] J.-M. Dums, H. Peurichard, M. J. Gomel, *J. Chem. Res. Synop.* **1978**, 54–57.
[7] T. Brinck, J. S. Murray, P. Politzer, *Int. J. Quantum Chem.* **1992**, *44*, 57–64.
[8] T. Brinck, J. S. Murray, P. Politzer, *Int. J. Quantum Chem.* **1993**, *48*, 73–88.
[9] T. Clark, M. Hennemann, J. S. Murray, P. Politzer, *J. Mol. Model.* **2007**, *13*, 291–296.
[10] B. Li, S. Q. Zang, L. Y. Wang, T. C. Mak, *Coord. Chem. Rev.* **2016**, *308*, 1–21.
[11] R. Bertani, P. Sgarbossa, A. Venzo, F. Lelj, M. Amati, G. Resnati, T. Pilati, P. Metrangolo, G. Terraneo, *Coord. Chem. Rev.* **2010**, *254*, 677–695.
[12] V. Amico, S. V. Meille, E. Corradi, M. T. Messina, G. Resnati, *J. Am. Chem. Soc.* **1998**, *120*, 8261–8262.
[13] P. Metrangolo, F. Meyer, T. Pilati, G. Resnati, G. Terraneo, *Angew. Chem. Int. Ed.* **2008**, *47*, 6114–6127; *Angew. Chem.* **2008**, *120*, 6206–6220.
[14] L. C. Gilday, S. W. Robinson, T. A. Barendt, M. J. Langton, B. R. Mullaney, P. D. Beer, *Chem. Rev.* **2015**, *115*, 7118–7195.
[15] M. R. Scholfield, C. M. V. Zanden, M. Carter, P. S. Ho, *Protein Sci.* **2013**, *22*, 139–152.
[16] D. Cappelletti, P. Candori, F. Pirani, L. Belpassi, F. Tarantelli, *Cryst. Growth Des.* **2011**, *11*, 4279–4283.
[17] S. L. Stephens, N. R. Walker, A. C. Legon, *J. Chem. Phys.* **2011**, *135*, 224309.
[18] H. I. Bloemink, J. H. Holloway, A. C. Legon, *Chem. Phys. Lett.* **1996**, *254*, 59–68.
[19] C. Domene, P. W. Fowler, A. C. Legon, *Chem. Phys. Lett.* **1999**, *309*, 463–470.
[20] E. A. Gillis, M. Demireva, M. G. Sarwar, M. G. Chudzinski, M. S. Taylor, E. R. Williams, T. D. Fridgen, *Phys. Chem. Chem. Phys.* **2013**, *15*, 7638–7647.
[21] A. C. Pearcy, K. A. Mason, M. S. El-Shall, *J. Phys. Chem. A* **2019**, *123*, 1363–1371.
[22] X. Zhang, G. Liu, S. Ciborowski, K. Bowen, *Angew. Chem. Int. Ed.* **2017**, *56*, 9897–9900; *Angew. Chem.* **2017**, *129*, 10029–10032.
[23] M. Jabłoński, M. Palusiak, *J. Phys. Chem. A* **2012**, *116*, 2322–2332.
[24] Y. X. Lu, J. W. Zou, Y. H. Wang, Y. J. Jiang, Q. S. Yu, *J. Phys. Chem. A* **2007**, *111*, 10781–10788.
[25] S. H. Jungbauer, S. Schindler, E. Herdtweck, S. Keller, S. M. Huber, *Chem. Eur. J.* **2015**, *21*, 13625–13636.
[26] R. Li, Q. Li, J. Cheng, Z. Liu, W. Li, *ChemPhysChem* **2011**, *12*, 2289–2295.
[27] A. Bauzá, I. Alkorta, A. Frontera, J. Elguero, *J. Chem. Theory Comput.* **2013**, *9*, 5201–5210.
[28] P. Politzer, J. S. Murray, *CrystEngComm* **2013**, *15*, 3145–3150.
[29] P. Politzer, J. S. Murray, *ChemPhysChem* **2013**, *14*, 278–294.
[30] C. E. Moore, *Natl. Stand. Ref. Data Ser.* (U.S. Natl. Bur. Stand.) **1971**, *NSRDS-NBS* 35, 208.
[31] A. Ding, J. Hesslich, *Chem. Phys. Lett.* **1983**, *94*, 54–57.
[32] A. T. Droege, P. C. Engelking, *Chem. Phys. Lett.* **1983**, *96*, 316–318.

Manuscript received: May 21, 2019
Accepted manuscript online: June 11, 2019
Version of record online: July 25, 2019

